HHS Public Access

Author manuscript

Lab Chip. Author manuscript; available in PMC 2015 June 21.

Published in final edited form as:

Lab Chip. 2014 June 21; 14(12): 2023–2032. doi:10.1039/c4lc00171k.

3D Printed Microfluidic Devices with Integrated Versatile and Reusable Electrodes

Jayda L. Erkal[a], **Asmira Selimovic**[b], **Bethany C. Gross**[a], **Sarah Y. Lockwood**[a], **Eric L. Walton**[a], **Stephen McNamara**[a], **R. Scott Martin**[b], and **Dana M. Spence**[a,*]

[a] Department of Chemistry, Michigan State University, 578 S. Shaw Lane, East Lansing, MI 48824

[b] Department of Chemistry, Saint Louis University, 3501 Laclede Ave, St. Louis, MO 63103

Abstract

We report two 3D printed devices that can be used for electrochemical detection. In both cases, the electrode is housed in commercially available, polymer-based fittings so that the various electrode materials (platinum, platinum black, carbon, gold, silver) can be easily added to a threaded receiving port printed on the device; this enables a module-like approach to the experimental design, where the electrodes are removable and can be easily repolished for reuse after exposure to biological samples. The first printed device represents a microfluidic platform with a 500 × 500 μm channel and a threaded receiving port to allow integration of either polyetheretherketone (PEEK) nut-encased glassy carbon or platinum black (Pt-black) electrodes for dopamine and nitric oxide (NO) detection, respectively. The embedded 1 mm glassy carbon electrode had a limit of detection (LOD) of 500 nM for dopamine and a linear response (R^2= 0.99) for concentrations between 25-500 μM. When the glassy carbon electrode was coated with 0.05% Nafion, significant exclusion of nitrite was observed when compared to signal obtained from equimolar injections of dopamine. When using flow injection analysis with a Pt/Pt-black electrode and standards derived from NO gas, a linear correlation (R^2 = 0.99) over a wide range of concentrations (7.6 - 190 μM) was obtained, with the LOD for NO being 1 μM. The second application showcases a 3D printed fluidic device that allows collection of the biologically relevant analyte adenosine triphosphate (ATP) while simultaneously measuring the release stimulus (reduced oxygen concentration). The hypoxic sample (4.76 ± 0.53 ppm oxygen) released 2.37 ± 0.37 times more ATP than the normoxic sample (8.22 ± 0.60 ppm oxygen). Importantly, the results reported here verify the reproducible and transferable nature of using 3D printing as a fabrication technique, as devices and electrodes were moved between labs multiple times during completion of the study.

Introduction

Electrodes have been successfully integrated with traditional polymer-based and glass-based microfluidic devices since the early 2000s.[1, 2] Polydimethylsiloxane (PDMS) – based

[*]**Corresponding Author Information:** Dana M. Spence 578 S. Shaw Lane East Lansing, MI 48824 Phone: 517-355-9715 ext.174 dspence@chemistry.msu.edu.

devices, either composed of all PDMS or PDMS-glass hybrids, are popular for integrating electrochemical detection in the microchip format due to its ease of fabrication and the ability of PDMS to seal (either reversibly or irreversibly) over the electrode of interest. A wide variety of techniques have been used to incorporate electrodes into these types of PDMS microfluidic devices including insertion of traditional wires/electrodes into the device,[3, 4] and use of screen-printed carbon ink electrodes,[5, 6] with the most popular method being fabrication of electrodes by sputtering/evaporation and photolithography.[7-11] Much of this early work drove development in electrophoresis-based detection of biologically relevant analytes such as catecholamines. While these devices have been used for a wide variety of applications including cellular analysis,[12] the utility of soft polymer devices suffers ultimately because of their lack of reusability. Irreversibly-sealed devices cannot be reused when a portion of the device fails. With reversibly sealed devices, most of the approaches to date do not permit the electrode to be repolished or regenerated for replicate experiments if the electrode is compromised. Biological studies typically require replicate experiments from multiple samples/subjects, so device-to-device (or electrode) reproducibility becomes a concern.

There has been an effort over the past few years to create reusable hybrid devices with conventional lithographic fabrication techniques. This effort includes reusable, hybrid devices fabricated from polystyrene[13-15] or polyester[16] as well as utilization of epoxy to embed electrodes.[17, 18] It has been shown that electrodes can be integrated in several of these substrates,[13, 14, 17, 18] with polishable electrodes. While more rugged and reusable than their polymer counterparts, the ease of customization and integration of these hybrid devices with commercial parts is still limited. For example, the PDMS layer of such a hybrid device can be integrated with a reusable epoxy or polystyrene base,[13] but the rigid, polystyrene layer still must be removed, cleaned, aligned, and resealed prior to use for additional experiments. The need to realign and reassemble devices contributes to reduced precision for biological studies requiring replicate studies and controls.

To date, in the chemical sciences, 3D printed devices have been utilized mostly for organic synthesis reactionware.[19-23] Applications in the biomedical fields include tissue scaffold development, [24-26] but the potential for the technology to significantly impact the field of microfluidics is high.[27, 28] We recently reported on the use of 3D printers to fabricate fluidic devices, with the printing of channels, integration of tubing to the device, and incorporation of a membrane above the channel in order to study drug transport and affect.[29] Other 3D printed devices have been utilized by the Spence laboratory to quantitatively investigate the properties of stored red blood cells for transfusion medicine.[30] The latter device utilized a circulating pumping scheme that could be disconnected prior to placement of the entire printed device into a commercial plate reader for quantitation of released cellular metabolites. In both of the reported studies, detection schemes were either optical or based on off-device mass spectrometric determinations. To date, integrated electrochemical detection schemes have not been reported with 3D printed devices. Here, we show that the integration of removable, reusable electrodes with 3D printed devices can be achieved by fabricating electrodes inside a commercial fitting whose dimensions are well documented and that can be easily transferred among labs. The use of commercially available components having defined and standardized dimensions is imperative because it enables

the fluidic device to be printed to accommodate such commercially defined parts. Importantly, the threaded functionality of the electrodes allows for ease of removal, repolishing, and reuse should the electrode become compromised, a significant advance for electrochemical detection in fluidic devices. For example, metal electrodes fabricated inside micron-sized polymer channels using deposition techniques can be used with biological samples, but cannot be reused. We present two 3D printed devices, one capable of housing electrodes (both working and reference) for electrochemical detection in 500 μm wide channels, and the other capable of analyte collection while simultaneously measuring oxygen concentration chronoamperometrically. The latter device was used to correlate the effect of oxygen tension on the release of ATP from red blood cells (RBCs) flowing through the channels of a printed device. Collectively, these studies demonstrate that different electrode materials can easily be introduced to the device. In fact, here, the limiting step to perform replicate experiments was the electrode and/or sample preparation rather than quality control of the microfluidic platform. Unlike traditional microfluidic devices, the technology can be shared via .STL files to promote standardization within the field.

Experimental

Materials

The following chemicals and materials were used as received: 0.5 mm gold wire, 0. 5 mm silver wire, firefly lantern extract, catechol, dopamine hydrochloride, chloroplatinic acid hydrate, lead (II) acetate trihydrate, Hanks' balanced salt solution (HBSS), TES (Trizma acetate, ethylenediaminetetraacetic acid (EDTA), sucrose) buffer, and potassium nitrate (Sigma Aldrich, St. Louis, MO); Armstrong C-7 resin, Activator A and E (Ellsworth Adhesives, Germantown, WI); silver conductive epoxy (MG Chemicals, Burlington, ON, Canada); J-B Kwik (J-B Weld Co., Sulphur Springs, TX); 250 and 500 μm platinum wire, 2 mm palladium wire, and 1 mm glassy carbon rod (Alfa Aesar, Ward Hill, MA); soldering wire and heat shrink tubes (Radio Shack); isopropanol and acetone (Fisher Scientific, Springfield, NJ); colloidal silver (Ted Pella, Redding, CA); electrode polishing pads (CH Instruments, Austin, TX; Allied High Tech Products, Inc., Rancho Dominguez, CA); nitric oxide (NO) tank (99.5%) (Airgas Inc., Radnor, PA); polyetheretherketone (PEEK) fitting nuts (P-131: 1/8" outer diameter (o.d.) tubing, P-137: 3/16" o.d. tubing), one-piece finger tight fittings for 1/16" o.d. tubing (IDEX Health & Science, Oak Harbor, WA); Nafion (5% w/w Nafion, Ion Power Inc., New Castle, DE or Sigma Aldrich, St. Louis, MO).

3D Printed Device Fabrication

Devices were designed in Autodesk Inventor Professional 2014 Student Edition. The part file was converted to an .STL file and was subsequently submitted for printing to the Department of Electrical and Computer Engineering at Michigan State University. The printer used was an Objet Connex 350 Multi-material 3D printer with VeroClear, which is a proprietary acrylate-based polymer material. The support material was cleared with compressed air. Further clearing of the support material was accomplished using polyimide-coated capillaries, compressed nitrogen, and sonication.

Electrode Fabrication

For the fabrication of epoxy-embedded electrodes in flangeless fitting nuts, electrode materials (250 and 500 μm platinum wire for platinum black; 1 mm glassy carbon rod and 2 mm palladium wire for glassy carbon) were cut to desired length (5 mm) and affixed, either by soldering or connection with colloidal silver, to a copper extending wire to provide the electrical connection. Heat shrink tubing was used to insulate the connection. The electrodes were inserted into the 1/8" o.d. PEEK fitting nut with serial alignment, such that sample first flowed over the working electrode. Following the assembly of the fitting nut and electrode, a thoroughly mixed combination of Armstrong C-7 adhesive (resin) and Armstrong Activator A was poured into the fitting and left to cure overnight. Later, the epoxy-filled fitting nut containing the electrodes was polished by wet polishing. For the fabrication of epoxy-embedded electrodes for oxygen detection, electrode materials (0.5 mm gold and 0.5 mm silver wire) were cut to desired length (5 mm) and affixed with conductive epoxy to a copper extending wire to provide the electrical connection. The connection was reinforced with J-B Kwik Weld. The electrodes were secured into the 3/16" o.d. PEEK fitting nut, and a thoroughly mixed combination of Armstrong C-7 adhesive (resin) and Armstrong Activator E was poured into the fitting and was left to cure overnight. The fabricated electrode was wet polished with P1000 grit sandpaper (3M, St. Paul, MN) to expose the electrodes and was subsequently polished with 0.05 μm alumina powder (CH Instruments).

Electrode Modification

For exclusion studies, Nafion coatings over the glassy carbon electrodes used for dopamine detection were prepared by physical deposition with 1 μL of a 0.05% Nafion solution (prepared in isopropyl alcohol from a 5% solution of commercially available Nafion) that was left to dry on the electrodes overnight. For the preparation of platinum black electrodes (250 μm Pt), the PEEK nut fitting containing the electrode and a Ag/AgCl reference were immersed in a 10 mL beaker filled with 3.5% chloroplatinic acid (w/v) and 0.005% lead (II) acetate trihydrate. Electrode plating was achieved by cycling the potential from +0.60 to 0.35 V (vs. Ag/AgCl) at a scan rate of 20 mV/s (1 scan).

The electrodes used for oxygen detection were polished before each use with 0.05 μm alumina powder, sonicated for 5-10 minutes, washed with deionized water, and placed in a 75 °C oven to dry for 10-15 minutes. After drying and cooling, the silver electrode was coated with AgCl using 3 M KCl (Fisher Scientific, Pittsburgh, PA), a 9 V battery with leads, and another Ag wire. After coating with AgCl, the electrodes were washed with deionized water and dried again. A Nafion coating was applied by dipping the electrodes into a 2.5% (for O_2 detection) w/w solution of Nafion diluted with isopropyl alcohol (prepared from a 5% w/w Nafion). The electrodes were dipped into the 2.5% Nafion solution and held for approximately 10 seconds until the electrodes were completely covered by solution. The electrodes were then allowed to dry on the bench top until ready for use in the printed device.

Flow Injection Analysis with a 3D Printed Device

The setup for flow injection analysis using PDMS devices and electrochemical detection has been previously reported.[6, 31, 32] In this study, a similar approach was taken, with the 3D

printed devices serving as the fluidic platform. In studies for Pt-black and glassy carbon electrode characterization, the device used contained a straight channel (500 μm width, 500 μm height, and 3 cm length). For characterization studies with the straight channel, the appropriate buffer was continuously pumped at 8.0 μL/min into the channel *via* a 500 μL syringe (SGE Analytical Science, Austin, TX) and a syringe pump (Harvard 11 Plus, Harvard Apparatus, Holliston, MA). The syringe was connected to 150 μm i.d. capillary tubing using a finger tight PEEK fitting and a luer adapter (Upchurch Scientific, Oak Harbor, WA). The same connectors and a 150 μm i.d. capillary fitted with a 350 μm o.d. PEEK tubing sleeve (Idex) were used to transition from a 4-port rotary injection valve (VICI Rotor, Valco Instruments, Houston, TX) to the device. The 4-port injection valve enabled reproducible 200 nL injections to the printed flow channel. Amperometric detection was performed with a 2-electrode system driven by potentiostat. The working electrode was glassy carbon, platinum, or platinum/platinum-black. Either palladium or platinum were used as the pseudo-reference electrode; both working and pseudo-reference electrodes were epoxy-embedded in a PEEK nut and fitted with the threads aligned with the 3D printed threaded port (i.e., not physically tapped) on the device. The PEEK nut was turned clockwise for tightening. A working electrode potential of +0.9 V (vs. Pt or Pd) was utilized for characterization studies using Pt, Pt-black, or glassy carbon.

HBSS and TES (pH 7.4) buffers were used, respectively, for characterization studies with NO and dopamine. For flow studies with NO, an NO standard stock solution (1.9 mM) was prepared by deoxygenating HBSS with Ar for 30 minutes, then saturating the solution with NO gas (99.5%) for 30 minutes.[33] The NO gas was purified before use by passing it through a column packed with KOH pellets to remove trace NO degradation products. Individual samples were made in deoxygenated volumetric flasks (sealed with suba seal) and deoxygenated HBSS.

Oxygen Standard Solutions

A calculation of oxygen standard concentrations was performed starting with Henry's Law, where the partial pressure of oxygen was assumed to be 0.20946 atm, and Henry's constant for oxygen was 769.23 atm/M. Air-purged and argon-purged solutions were prepared by sparging compressed air or argon into HBSS in a 100 mL round bottom flask for at least 30 minutes. Oxygen standards were prepared by mixing measured volumes of air-purged HBSS (saturated) and argon-purged HBSS (deoxygenated) in a 500 μL syringe. The oxygen concentrations of both air- and argon-purged buffers were confirmed with a commercial oxygen probe (Symphony SP70D, VWR). The argon-purged and air-purged solution oxygen concentrations did not differ significantly from the calculated values using Henry's constant. To prepare oxygen standard solutions with RBCs, the two argon-purged and air-purged buffers were added to the syringe first, and then packed RBCs were added to the syringe at an appropriate volume to create a 7% solution of RBCs.

RBC Purification

Blood collection procedures were approved by the Biomedical, Health Sciences Institutional Review Board (BIRB) at Michigan State University. Human whole blood was obtained by venipuncture from informed, consenting donors and was collected into 10 mL Vacutainer

tubes coated with lithium heparin (BD Biosciences, San Jose, CA) to prevent coagulation. RBCs were initially separated from the plasma and buffy coat by centrifuging the whole blood at 500 *g* at 25°C for 10 minutes. The supernatant and buffy coat were removed by aspiration, and the RBCs were washed with HBSS and centrifuged again at 500 *g* for 10 minutes. This process was repeated twice more for a total of three washes with HBSS. The hematocrit of the purified RBCs was determined with a StatSpin CritSpin micro-hematocrit centrifuge (Iris Sample Processing, Inc., Westwood, MA).

Chronoamperometric Oxygen Measurements

Electrochemical measurements of oxygen were performed using a commercially available potentiostat (CH Instruments). The 3D printed device hosting the electrodes used for oxygen detection had a channel measuring 7 mm in length, 3 mm in width, and 0.5 mm in height. The device contained a threaded electrode port for the gold and Ag/AgCl electrode. The 3/16" nut housing the electrodes was screwed into the threaded port, and the electrodes were attached to the potentiostat via leads. Flow of oxygen standards with or without 7% RBCs (6 μL/min) from 500 μL syringes was controlled using a syringe pump (Harvard). Samples were interfaced to the device through segments of 50 μm i.d. capillary tubing and the same finger tight fittings and luer locks described above. Unless otherwise specified, parameters for chronoamperometric measurement of oxygen are as follows: Initial V: 0 V; High V: 0 V; Low V: -1 V; Initial step polarity: negative; Number of steps: 2;

Pulse width: 1 s; Sample interval: 0.001 s; Quiet time: 2 s; Sensitivity (A/V): 1×10^{-5}. Calibration curves were generated using current values at 0.3 seconds from the chronoamperograms.

ATP Detection

Transwell membrane inserts (polyester, 0.4 μm pores, Corning, Corning, NY) were inserted into the well ports in the 3D-printed device. The well inserts were filled with 200 μL of HBSS, and stable RBC flow (6 μL/min) was established, i.e., no air bubbles. The wells were covered with a wet Kim-wipe to minimize evaporation from wells, and the 7% RBCs were allowed to flow for 20 minutes. Next, the HBSS in the wells was collected into 600 μL posi-click tubes (Denville Scientific, South Plainfield, NJ), which were stored on ice until all samples were pumped through the device. 50 μL of each sample were plated in triplicate on a 96-well plate. A luciferin luciferase mixture was prepared by adding 2 mg D-Luciferin (GoldBio, St. Louis, MO) to 5 mL of distilled, deionized water (DDW). This 5 mL mixture was added to a vial of firefly lantern extract, which was shaken until solids were dissolved. The mixture was divided into 100 μL aliquots and frozen for storage. Aliquots were thawed and diluted 1:1 with HBSS on the day of the experiment. To measure the RBC-derived ATP in the transwell inserts, 50 μL of the luciferin luciferase mixture were pipetted with a multichannel pipette into the wells, and the resulting chemiluminescence was immediately read with a commercial plate reader (SpectraMax M4, Molecular Devices, Sunnyvale, CA).

Imaging

Color images, with the exception of the image shown in Figure 1C and 6B, were captured with an upright Olympus, BX51 microscope equipped with an Infinity3 camera (Hitschfel Instruments, Inc).

Black and white non-fluorescent images were obtained from a stereoscope (Olympus SXZ12) operating in bright field mode using a Sony 3CCD color camera (Leeds Precision Instruments, Minneapolis, MN). The black and white non-fluorescent images in Figures 4 and 5 were captured with an upright fluorescence microscope using the bright field setting with a CCD camera (Olympus MVX10).

Results and Discussion

Standardization of Devices Between Labs

The use of parts with defined dimensions was essential in that the fluidic device was fabricated to accommodate the commercial part. That is, the choice of electrode housing (PEEK nuts) for these studies, in part, drove the 3D device design. It was important that the electrode housings had fixed outer diameters, while the interior diameters could vary, depending on the size of electrodes to be incorporated. Secondly, it was important that the electrode housings have threads so they could be easily removable. More importantly, the threads were of the same standard type, i.e., 5/16-24, for the two types utilized in this study, allowing the electrodes to be used interchangeably between devices, if necessary. These properties of the electrode housings allowed printing of an electrode port in both 3D devices that could be used with various models of nuts because both parts had the same outer diameter and threading. The only difference between the housings was the internal diameter; this difference enabled the authors take liberty in the choice of electrode wire diameters and in the electrode alignment with channels, particularly in the 500 μm wide channel device. The nut used for fabrication of glassy carbon and Pt-black electrodes was the P-131 model, while the P-137 model was used for the gold and Ag/AgCl electrode. This standardization of the electrode port allowed for the electrodes of varying materials to be made in different labs. The microfluidic device used for characterization studies for glassy carbon and Pt-black was printed at Michigan State University and was shipped to the Martin lab at Saint Louis University for collaboration. The fact that a device can be made in one lab and utilized in another demonstrates the transferability when using 3D printed devices. Although the transferability of the .STL file between academic laboratories is expected to ease fabrication requirements, the variety of printable materials and printing techniques are two factors that will create challenges for researchers. These two factors can impact the dimensions and ultimately the functionality of a printed device or part. This is due to the variation in resolution and in printer types (stereolithography, fused deposition modeling, etc.) and also in the desired materials' physical properties.

Integration with Microfluidic Channels

Devices were designed and modified in Autodesk software using the dimensions of the above-mentioned, commercially available fittings. For the devices presented herein, dimensions in the part files were set and iteratively corrected using both part dimensions

provided by the supplier and also by manually measuring with calipers. Devices required multiple iterations to achieve acceptable contact points for inlets/outlets, well inserts and electrode ports. It is also worth mentioning that if a different material for the device is desired, this iterative process must be repeated for printing with a different material. This is due to differences in material properties that result from changes in material composition as well as the printer type. For example, a device printed in one material will not have exactly the same dimensions as the same device printed in another material, even with the same printer, because of changes in the material properties. The dimension precision, which is termed tolerance by the 3D printing community, is estimated to be on the order of tenths of millimeters. However, this has yet to be investigated thoroughly for the devices reported here.

Electrode alignment in the 500 μm channel device was achieved by sanding the PEEK nut to remove threading until the electrodes were flush with the channel when the nut was fully tightened, ensuring the same alignment each time the electrode was used. While this method worked well for these studies, it is anticipated that in future fabrication, alignment of the electrodes with channels can be addressed in the design process with the CAD program (by integrating the electrode nut and device together in the part file to check alignment) or in the fabrication step. For example, fabrication of working and counter/reference wires in separate, smaller diameter 3D printed fittings that are geometrically directly opposed in the channel would not only ease fabrication requirements, but also allow for better control over electrode placement. Separate alignment of electrodes could be spatially more practical for experimental design, but more importantly it could also minimize the dead volume associated with connections to the device. The dead volume in these two devices was not observed to interfere significantly with the electrochemical measurements. The calculated dead volume for the inlet, obtained by using measured distances with calipers, was estimated to be about 0.13 μL, assuming the area between the fitting end and the beginning of the channel was conical in shape due to mismatch between the fitting and conical inlet. This volume constitutes approximately 3.3% of the total volume of the 500 μm device (3.9 μL). It is difficult to estimate the dead volume in the electrode fitting and in the membrane area by measuring with calipers due to visual obstruction by the fitting and membrane. However, no deleterious effects, such as band broadening or peak splitting, were observed due to dead volume in the flow injection analysis or chronoamperometric data.

Channel widths in the presented devices are either 0.5 mm or 3 mm. Devices with 250 μm and 100 μm wide channels were printed, but fluid flow was obstructed by the un-removed support material that was present in the channel post-print. Currently, removal of support material is accomplished using compressed air, sonication, and scraping. This limits the use of sub-500 μm in width channels for this study, as it becomes difficult to clear support material out of smaller dimension channels. However, it is anticipated that as polishing techniques, both physical and chemical in nature, for these cured acrylate-based materials improve, sub 500 μm features will become possible to fabricate consistently.

Fabrication and Characterization of Glassy Carbon and Pt-black

For the first time, electrode materials were integrated with a 3D printed microfluidic device (500 μm channel width) to enable electrochemical detection of electroactive species, in this case dopamine and NO (Figure 1). The same physical device was used with both glassy carbon and Pt-black electrodes. This was possible because the electrode housing was a standard 5/16-24 threaded fitting, which allows for any fitting with the appropriate diameter and threading to be integrated with the device. Parts A & B in Figure 1 show the Autodesk rendering of the device, where threads and channel can be visualized in three dimensions. This visualized file is termed the part file and is the precursor to the .STL file submitted for printing. Figure 1C is a micrograph of the threaded epoxy-embedded electrodes aligned in the center of the 500 μm channel. Part D in Figure 1 shows the assembled device with commercial fittings, electrode, and electrode leads. This setup is interfaced with a syringe pump and with a 4-port injection valve with a loop volume of 250 μL.

A major application of microfluidic-based electrochemical detection is monitoring neurotransmitters; therefore, the integration of commonly used carbon electrodes for catecholamine detection was demonstrated. Specifically in these studies, a glassy carbon working electrode (1 mm diameter) was utilized to detect dopamine. When utilized with flow injection analysis, the embedded 1 mm glassy carbon electrode could measure a 500 nM limit of detection (LOD) for dopamine in the 500 μm channel device with linear response ($R^2 = 0.99$) for a wide range of concentrations (25-500 μM).

Electrode modifications, such as a coating with a perm-selective membrane like Nafion to selectively permit neutral or positive small molecules to the electrode, are widely used to make electrodes more selective toward an electroactive species.[34, 35] To investigate the use of Nafion for selectivity, the glassy carbon electrode was coated with a 0.05% Nafion solution and was used for flow injection analysis. As can be seen in Figure 2, significant exclusion of 100 μM nitrite was achieved with the Nafion-coated electrode (average peak height = 0.31 ± 0.02 nA, n = 3) when compared to signal obtained from equimolar injections of dopamine over the same electrode (average peak height = 1.83 ± 0.06 nA, n = 3, see Figure 2, panel B) and nitrite over an unmodified electrode (average peak height = 2.80 ± 0.02 nA).

Platinum electrodes are commonly used for NO detection[36] and can be made more sensitive for NO with the use of platinized electrodes.[37] In the platinization process, a chloroplatinic acid solution, which contains a small amount of lead acetate, is used to electrochemically deposit black particles of platinum onto the platinum working electrode. The optimal deposition cycle to be used for NO detection in microfluidic devices has previously been determined.[38] Figure 3 illustrates a bare 500 μm Pt electrode (used as the pseudo-reference) and the Pt-black surface modification on the 250 μm platinum working electrode. To demonstrate the signal enhancement resulting from the Pt-black deposition on platinum, repeated injections of a 190 μM NO solution were analyzed with a bare Pt or Pt-black electrode. As shown in Figure 3, a nearly 7-fold signal increase was observed for NO detection with the Pt-black modified platinum electrode (average peak height = 3.61 ± 0.02 nA, n = 3) relative to a bare platinum electrode (average peak height = 0.54 ± 0.06 nA, n = 3). Others have previously reported similar values in signal enhancement (8-13 times signal

amplification) when using Pt-black electrodes for NO detection in studies not involving microfluidic devices.[37] When using flow injection analysis and standards derived from NO gas, the 250 μm platinum electrode modified with Pt-black exhibited a reproducible response (RSD = 4.2%, n=12) (average peak height = 2.63 ± 0.11 nA, n=12). An NO calibration curve for this electrode demonstrated a linear correlation (R^2 = 0.99) over a wide range of concentrations (7.6 - 190 μM). The LOD for NO on this Pt-black electrode was 1 μM.

Fabrication and Integration of Gold and Ag/AgCl Electrodes for Oxygen Detection in Biological Samples

Clark-type electrodes, using platinum,[39, 40] silver[41, 42] or gold[43-45] working electrodes, are commonly used for measuring dissolved oxygen in biological samples. To determine if Nafion-coated gold and Ag/AgCl electrodes (Figure 4A), fabricated and modified as described above, were suitable for oxygen detection in 7% RBCs in the 3D printed device, oxygen standards in the presence and absence of 7% RBCs were measured (Figure 4B). The device for this characterization contained a channel 3 mm in width, 0.5 mm in height and a threaded inlet, outlet, and electrode port. The 3 mm wide channel dimension was chosen to accommodate both the 0.5 mm electrodes as well as the transwell membrane inserts for the studies described below. After confirmation that the electrode response had a linear relationship with oxygen concentration (Figure 4B), the device part file was modified to include two wells to house membrane inserts and was resubmitted for printing, resulting in the device displayed in Figure 5. This modification step took significantly less time (hours) than traditional lithographic techniques, which would require creation of a new master (at least 1 day). Three electrodes were fabricated for oxygen detection and were used to collect the chronoamperometric data. The average signal from the three electrodes for an 8.74 ppm oxygen standard with 7% RBCs was 0.83 μA, and the standard deviation was 0.10 μA, resulting in an RSD of 12%.

Electrochemical Detection of Oxygen in a Stream of Flowing Hypoxic RBCs Using a 3D Printed Device

The electrochemical and fluorescence detection of biologically relevant analytes in microfluidic devices has been previously reported.[46-48] Here, we demonstrate the amenability of a rigid, 3D printed device for electrochemical detection of oxygen in a stream of flowing hypoxic RBCs, while simultaneously collecting the ATP released from these cells in a transwell insert incorporated into the device. This device (Figures 5 and 6) facilitated measurement of these two analytes by including a threaded port (5/16-24 threading) for the removable Nafion-coated gold and Ag/AgCl electrode and two wells to house membrane inserts (0.4 μm pores). The electrode was used to chronoamperometrically measure the oxygen tension in a flowing stream of RBCs, while the membrane inserts were used to simultaneously collect ATP release for off device chemiluminescence detection, as described above. ATP release from flowing normoxic RBCs (8.22 ± 0.60 ppm oxygen) and from flowing hypoxic RBCs (4.76 ± 0.53 ppm oxygen) was compared. Raw chemiluminescence intensity values from triplicate normoxic and hypoxic samples were averaged, and the values were normalized to the normoxic sample values. The normalized

data are presented in Figure 6C. The hypoxic RBC samples released on average 2.37 ± 0.37 times more ATP than the normoxic RBC samples.

Previous work from the Spence group[49, 50] has focused on measuring metabolite release from hypoxic RBCs to determine the underlying mechanism and biological importance of hypoxia-induced vasodilation. An attractive property of the acrylate-based printing material is its low permeability to oxygen. In the above oxygen measurements, it was desired that the device material not be as permeable to oxygen as compared to PDMS in order to minimize the background signal at the Nafion-coated electrodes. A rigid, 3D printed device that can be sterilized using traditional methods (rinsing with ethanol), reused as desired, and coupled with various electrode materials and well inserts that are amenable to cell culture, is an attractive platform for more complex biological studies.

Conclusions

3D printing is a fabrication method that can be used to print rigid, reusable fluidic devices. In this paper, we were able to show that a variety of electrode materials (carbon, platinum, gold, silver) for a wide range of applications (neurotransmitter detection, NO detection, measuring oxygen tension in a stream of red blood cells) can be easily integrated into these devices along with other functionalities such as fluidic interconnects and membrane inserts to enable signaling molecule detection (ATP via chemiluminescence). Because of the dimensional control that computer-aided design (CAD) programs allow, these devices can be easily integrated with commercially available parts whose dimensions are known or can be measured. This enables a module-like approach to experimental design, allowing a researcher to fabricate a multicomponent device, troubleshoot any problems, modify or add to the part file, and reprint for continued study – all on a similar or faster time scale than with photo- and soft lithographic techniques. Unlike the physical format of soft lithographic masters, the part files for 3D printing are standardized, i.e., the part can be exchanged with and transferred to any lab that has access to a CAD program and 3D printer. Importantly, the electrode fitting is removable and reusable, a significant improvement over the traditional one-time-use evaporation/deposition-based metal electrodes. This technology has the potential to not only change the way that researchers approach collaboration but also our perceived limitations of experimental designs, particularly in biological studies where spatial control of samples or cells is critical.

Acknowledgements

The authors would like to acknowledge Brian Wright in the Department of Electrical and Computer Engineering at Michigan State University for his continued help with 3D printing. This work was funded by NIH (Grant# 1R21EB016379).

References

1. Martin RS, Gawron AJ, Lunte SM, Henry CS. Anal Chem. 2000; 72:3196–3202. [PubMed: 10939387]
2. Woolley AT, Lao K, Glazer AN, Mathies RA. Anal. Chem. 1998; 70:684–688. [PubMed: 9491753]
3. Vickers JA, Henry CS. Electrophoresis. 2005; 26:4641–4647. [PubMed: 16294295]
4. Gawron AJ, Martin RS, Lunte SM. Electrophoresis. 2001; 22:242–248. [PubMed: 11288891]

5. Kovarik ML, Li MW, Martin RS. Electrophoresis. 2005; 26:202–210. [PubMed: 15624172]
6. Kovarik ML, Torrence NJ, Spence DM, Martin RS. Analyst. 2004; 129:400. [PubMed: 15116230]
7. Castle PJ, Bohn PW. Anal Chem. 2004; 77:243–249. [PubMed: 15623302]
8. Bowen AL, Martin RS. Electrophoresis. 2010; 31:2534–2540. [PubMed: 20665914]
9. Lacher NA, Lunte SM, Martin RS. Anal. Chem. 2004; 76:2482–2491. [PubMed: 15117187]
10. Amatore C, Da Mota N, Lemmer C, Pebay C, Sella C, Thouin L. Anal. Chem. 2008; 80:9483–9490. [PubMed: 19007242]
11. Manica DP, Mitsumori Y, Ewing AG. Anal. Chem. 2003; 75:4572–4577. [PubMed: 14632066]
12. Johnson AS, Selimovic A, Martin RS. Anal Bioanal Chem. 2013; 405:3013–3020. [PubMed: 23340999]
13. Johnson AS, Anderson KB, Halpin ST, Kirkpatrick DC, Spence DM, Martin RS. Analyst. 2013; 138:129–136. [PubMed: 23120747]
14. Anderson KB, Halpin ST, Johnson AS, Martin RS, Spence DM. Analyst. 2013; 138:137–143. [PubMed: 23120748]
15. Dusseiller MR, Schlaepfer D, Koch M, Kroschewski R, Textor M. Biomaterials. 2005; 26:5917–5925. [PubMed: 15949557]
16. Fiorini GS, Lorenz RM, Kuo JS, Chiu DT. Anal Chem. 2004; 76:4697–4704. [PubMed: 15307779]
17. Johnson AS, Selimovic A, Martin RS. Electrophoresis. 2011; 32:3121–3128. [PubMed: 22038707]
18. Selimovic A, Johnson AS, Kiss IZ, Martin RS. Electrophoresis. 2011; 32:822–831. [PubMed: 21413031]
19. Dragone V, Sans V, Rosnes MH, Kitson PJ, Cronin L. Beilstein Journal of Organic Chemistry. 2013:9.
20. Kitson PJ, Rosnes MH, Sans V, Dragone V, Cronin L. Lab Chip. 2012; 12:3267–3271. [PubMed: 22875258]
21. Kitson PJ, Symes MD, Dragone V, Cronin L. Chemical Science. 2013; 4:3099–3103.
22. Mathieson JS, Rosnes MH, Sans V, Kitson PJ, Cronin L. Beilstein Journal of Nanotechnology. 2013; 4:285–291. [PubMed: 23766951]
23. Symes MD, Kitson PJ, Yan J, Richmond CJ, Cooper GJT, Bowman RW, Vilbrandt T, Cronin L. Nature Chemistry. 2012:4.
24. Antonov EN, Bagratashvili VN, Whitaker MJ, Barry JJA, Shakesheff KM, Konovalov AN, Popov VK, Howdle SM. Advanced materials. 2005; 17:327–330. [PubMed: 17464361]
25. Lam CXF, Mo X, Teoh S-H, Hutmacher D. Materials Science and Engineering: C. 2002; 20:49–56.
26. Lee M, Wu BM. Methods in Molecular Biology. 2012; 868:257–267. [PubMed: 22692615]
27. Gross BC, Erkal JL, Lockwood SY, Chen C, Spence DM. Anal Chem. 2014:140116094947007.
28. Waldbaur A, Rapp H, Lange K, Rapp BE. AnalMethods-Uk. 2011; 3:2681–2716.
29. Anderson KB, S.Y. L, Martin S, Spence DM. Anal Chem. 2013; 85:5622–5626. [PubMed: 23687961]
30. Chen C, Wang Y, Lockwood SY, Spence DM. Analyst (Cambridge, United Kingdom). 2014 In Revision.
31. Batz NG, Martin RS. Analyst. 2009; 134:372. [PubMed: 19173065]
32. Hulvey M, Martin R. Chem. Educator. 2004; 9:1–7.
33. Shin JH, Privett BJ, Kita JM, Wightman RM, Schoenfisch MH. Anal Chem. 2008; 80:6850–6859. [PubMed: 18714964]
34. Kristensen EW, Kuhr WG, Wightman RM. Anal Chem. 1987; 59:1752–1757. [PubMed: 3631500]
35. Zimmerman JB, Wightman RM. Anal Chem. 1991; 63:24–28. [PubMed: 1810167]
36. Shibuki K. Neuroscience Research. 1990; 9:69–76. [PubMed: 2175870]
37. Lee Y, Oh BK, Meyerhoff ME. Anal Chem. 2003; 76:536–544. [PubMed: 14750844]
38. Selimovic A, Martin RS. Electrophoresis. 2013; 34:2092–2100. [PubMed: 23670668]
39. Jobst G, Urban G, Jachimowicz A, Kohl F, Tilado O, Lettenbichler I, Nauer G. Biosensors and Bioelectronics. 1993; 8:123–128.

40. Clark LC, Lyons C. Annals of the New York Academy of Sciences. 1962; 102:29–45. [PubMed: 14021529]
41. Yang Z, Sasaki S, Karube I, Suzuki H. Anal Chim Acta. 1997; 357:41–49.
42. Suzuki H, Hirakawa T, Watanabe I, Kikuchi Y. Anal Chim Acta. 2001; 431:249–259.
43. Maclay GJ, Buttner WJ, Stetter JR. IEEE Transactions on Electron Devices. 1988; 35:793–799.
44. McLaughlin GW, Braden K, Franc B, Kovacs GTA. Sensors and Actuators B: Chemical. 2002; 83:138–148.
45. Lee J-H, Lim T-S, Seo Y, Bishop PL, Papautsky I. Sensors and Actuators B: Chemical. 2007; 128:179–185.
46. Lapos JA, Manica DP, Ewing AG. Anal Chem. 2002; 74:3348–3353. [PubMed: 12139039]
47. Wang J, Pumera M. Anal Chem. 2002; 74:5919–5923. [PubMed: 12498184]
48. Kisler K, Kim BN, Liu X, Berberian K, Fang Q, Mathai CJ, Gangopadhyay S, Gillis KD, Lindau M. Journal of biomaterials and nanobiotechnology. 2012; 3:243. [PubMed: 22708072]
49. Halpin ST, Spence DM. Anal. Chem. (Washington, DC, U. S.). 2010; 82:7492–7497.
50. Faris A, Spence DM. Analyst. 2008; 133:678–682. [PubMed: 18427692]

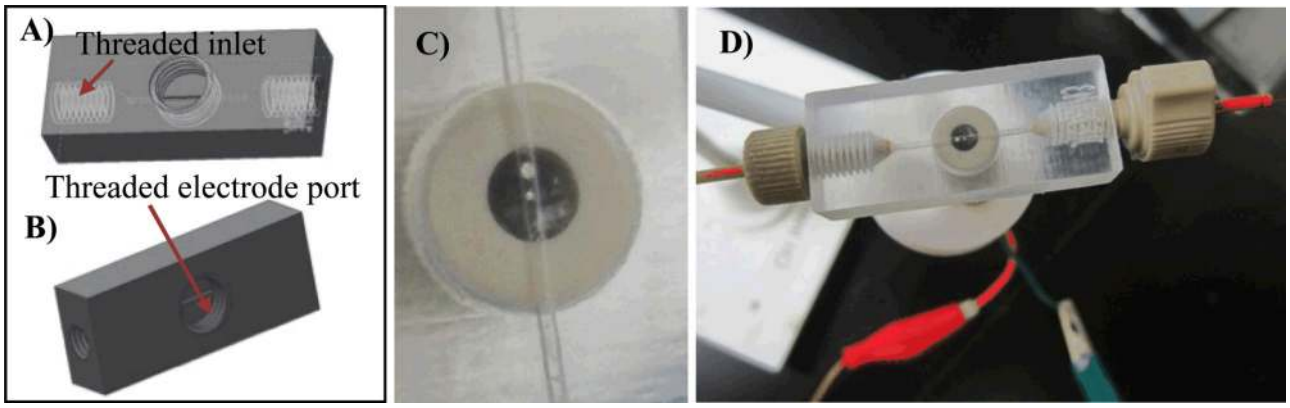

Figure 1.

3D device used for electrochemical detection. A-B) 3D renderings of the device in Autodesk software; C-D) Printed 0.5 mm-wide channel device in VeroClear material. The Pt-electrode is screwed into the electrode port, showing alignment of both Pt wires with the 0.5 mm channel (panel C). In panel D, the device is shown with the Pt-electrode, electrode leads, and the fittings used to integrate the device with a syringe pump.

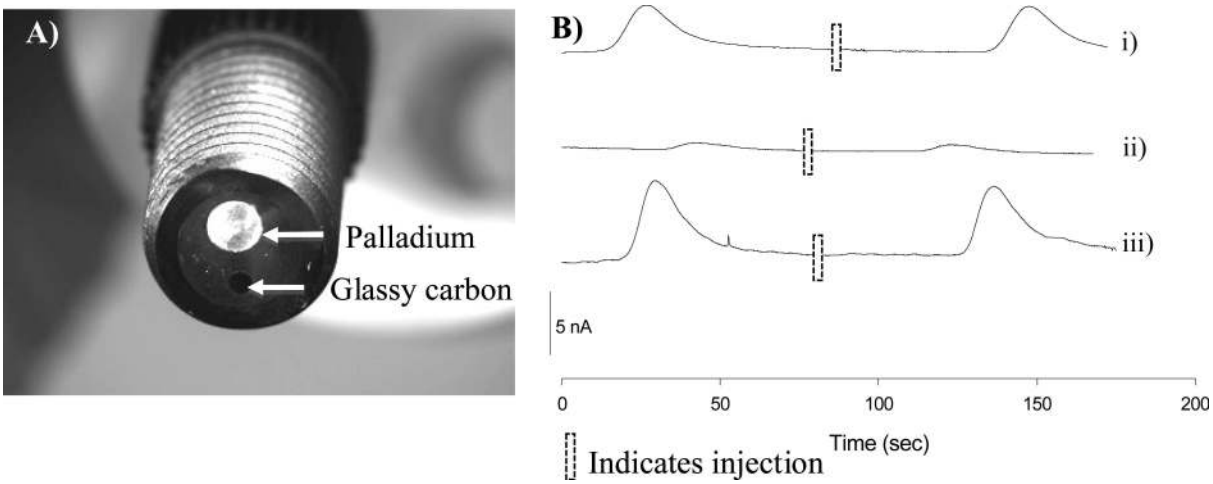

Figure 2.

Glassy carbon working electrode for the detection of dopamine. A) Image showing the flangeless fitting with a 2 mm palladium pseudo-reference and a 1 mm glassy carbon working electrode; B) flow injection analysis to show selectivity of a Nafion-coated glassy carbon electrode; i) Response for dopamine [100 μM] using the Nafion-coated glassy carbon electrode; ii) Response for nitrite [100 μM] using the Nafion-coated glassy carbon electrode; iii) Response for nitrite [100 μM] using a non-modified glassy carbon electrode.

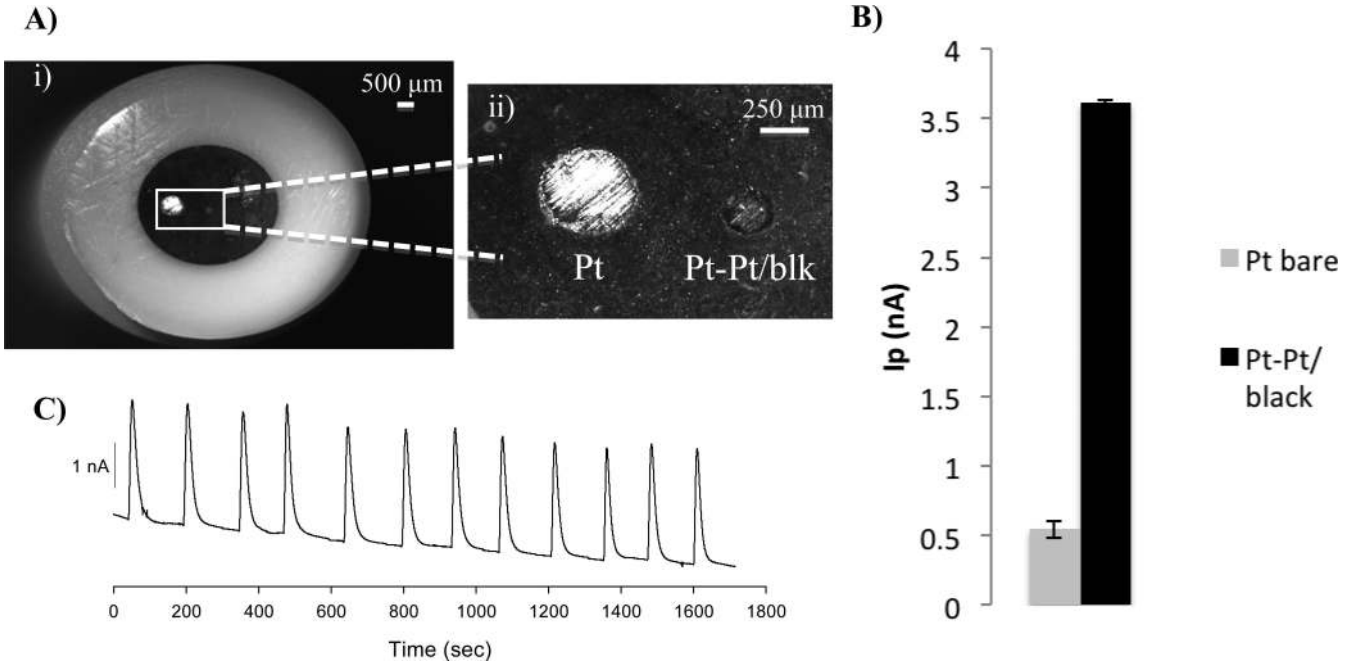

Figure 3.

Platinum electrodes for NO detection. A) i) Platinum pseudo-electrode (500 μm) and platinum working electrode [250 μm] encapsulated with epoxy in a flangeless fitting; ii) Zoomed micrograph of the platinum black modified platinum working electrode; B) Bar graph comparing the signal for NO [190 μM] with a bare Pt electrode verses the Pt/Pt-black modified electrode; C) Amperogram of reproducible 190 μM NO injections over the Pt/Pt-black electrode.

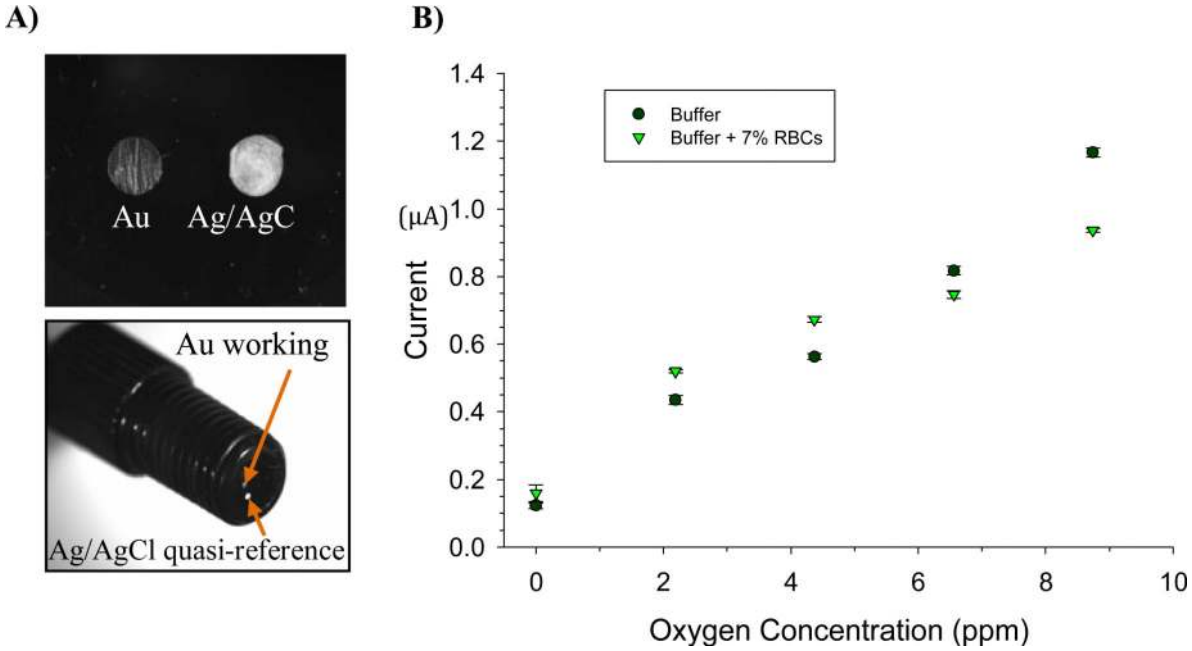

Figure 4.

Measuring O_2 tension in a flowing stream of buffer (HBSS) and in HBSS with RBCs. Measurements were made with a Nafion-coated gold electrode and Ag/AgCl quasi-reference electrode. A) Micrographs of the electrode containing gold and silver wire secured with C-7 epoxy. In both micrographs, the silver wire is coated with AgCl; B) Calibration curve data for oxygen standards in HBSS [$y=1.13\times10^{-7}x+1.26\times10^{-7}$; $R^2 = 0.98$] and in the presence of RBCs [$y=8.15\times10^{-8}x+2.50\times10^{-7}$; $R^2 = 0.93$]. N = 1 electrode with triplicate measurement. Error = standard deviation.

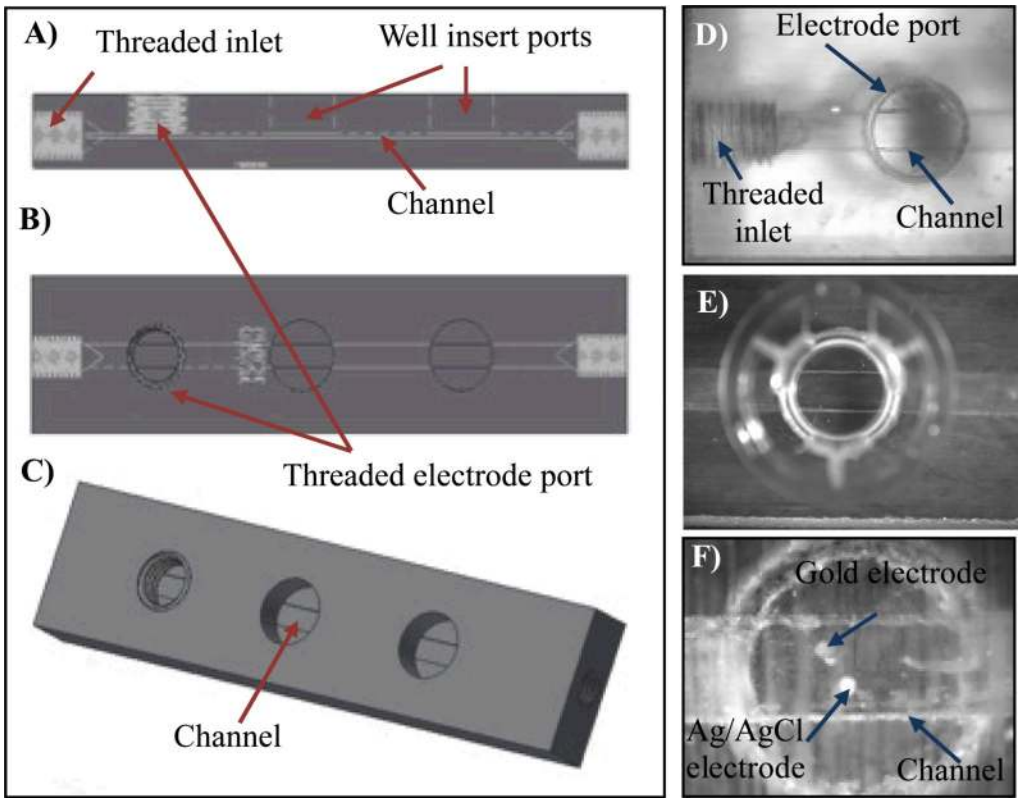

Figure 5.

Fabrication of 3D device to measure oxygen and ATP from flowing RBCs. The left side of the figure shows the rendering of the device in the Autodesk software. A) Side profile of device detailing the threaded inlet, electrode port, and well insert ports; B) Top view of device; C) Solid body view of device; D) 3D printed device in VeroClear material, detailing the inlet and electrode port; E) Transwell membrane inserted into the device via the well insert port; F) 3D printed device with electrode inserted fully into the port, showing the working and quasi-reference electrodes for oxygen sensing.

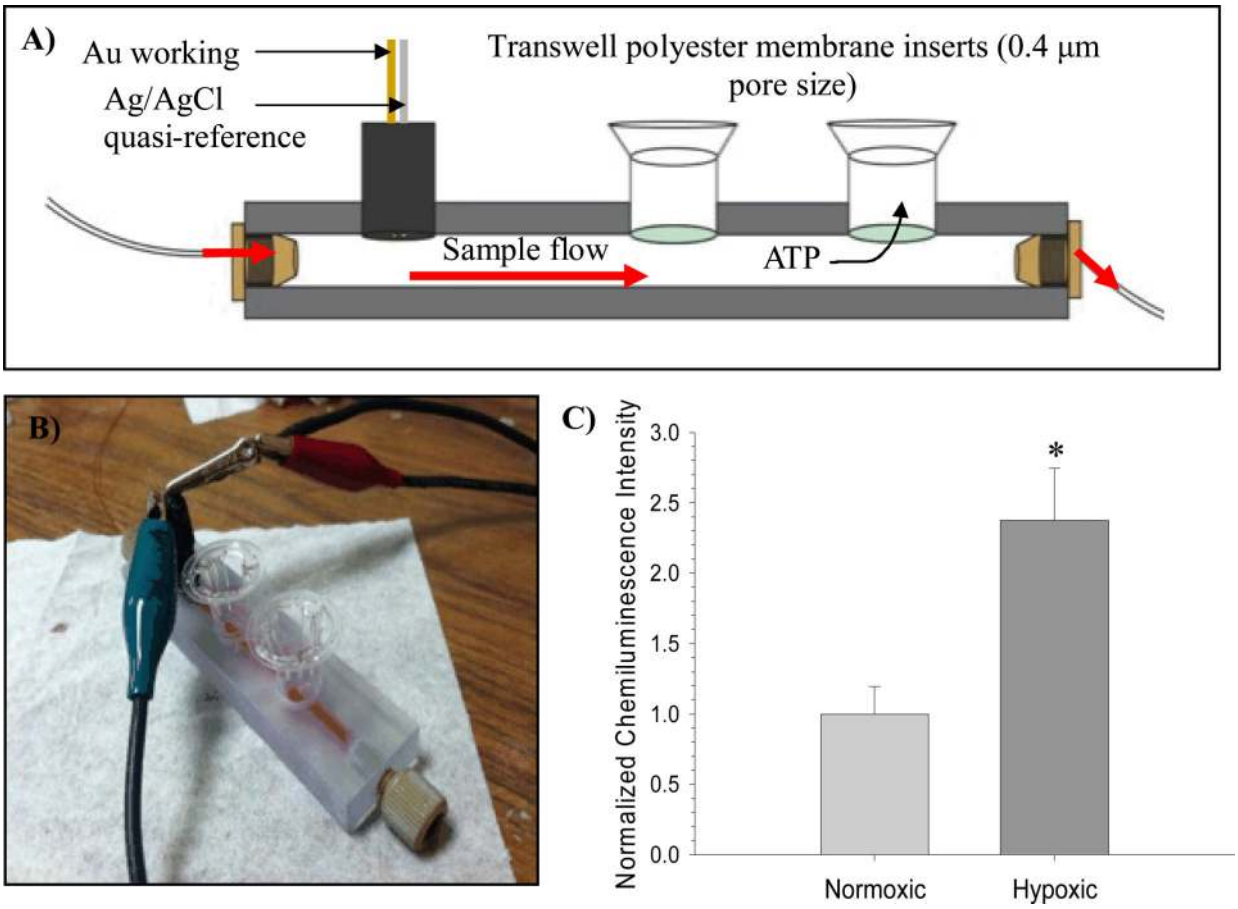

Figure 6.

Fluidic device for correlation of oxygen tension and ATP release. A) Schematic of device; B) Picture of the assembled device with RBCs being pumped through the system; C) Comparison of RBC ATP release from a normoxic sample (8.22 ± 0.60 ppm oxygen) to a moderately hypoxic sample (4.76 ± 0.53 ppm oxygen). N = 3 donors; error = s.e.m., * $p < 0.05$.